Comparison of the hardening behaviour of different steel families: from Mild and Stainless Steel to Advanced High Strength Steels

E. Silvestre[1*], J. Mendiguren[1], L. Galdos[1], E. Sáenz de Argandoña[1]

[1]*Mondragon University, 4 Loramendi, 20500, Mondragon, Spain*

Abstract

Although steel has been used in vehicles from the automotive industry's inception, different steel grades are continually being developed in order to satisfy new fuel economy requirements. For example, advanced high strength steel grades (AHSS) are widely used due to their good strength/weight ratio. Because each steel grade has a different microstructure composition, they show different behaviours when they are subjected to different strain path in forming processes. Materials with high yield strength tend to be influenced by phenomena of cyclic plasticity such as the Baushchinger Effect, while low yield strength materials tend to harden when they are subjected to cyclic loading.

Different steel grades are used in different forming processes, which are usually optimized by numerical tools such as Finite Element Models. This method requires proper hardening rules in order to correctly predict the real behaviour of the materials. For instance, AHSS are usually well modeled by means of mixed isotropic-kinematic hardening models.

The methodology for developing a mixed hardening model to be implemented in finite element codes and simulate sheet forming processes requires three steps: (i) an appropriate experimental test to obtain stress-strain curves, (ii) a model able to predict accurately the behaviour of the material and (iii) a parameter identification method. Currently, there are few studies which analyse and model the hardening behaviour of different steel families following the same methodology. In this work, a wide range of steels from low to high yield strengths were characterized and their hardening behaviour modeled with the same methodology so as to provide comparative data.

In particular, the Chaboche and Lemaitre hardening model was successfully fitted to the experimental stress-strain curves obtained from a tension-compression test. The test was performed at low cyclic deformations (±2%) due to the limitation of the test to achieve higher deformations during the compression without buckling. Therefore, this modelization is useful for low deformation processes such as the roll leveling process (Silvestre et al. 2013, Silvestre et al. 2012), in which the maximum deformations achieved are lower than 2 %.

Keywords: Cyclic hardening, Bauschinger effect, Mixed hardening law, Parameter identification

1. Introduction

In recent years, the development of new steel grades with high performance has been driven by new requirements in the automotive industry. Reducing the weight of a vehicle is a straightforward strategy to improve fuel economy, but it can potentially create safety problems. For that reason, efforts have been concentrated on the development of new steel grades with a competitive strength/weight ratio [1]. However, the development of these materials leads to the apparition of undesirable phenomena during forming process which affect the quality of the final product [2]. For example, new high strength steels (HSS) and advanced high strength steel (AHSS) grades satisfy the mechanical properties required for an adequate design, i.e. durability, strength, stiffness, good crash energy absorption, acoustic properties, low production costs compared with other materials and the possibility of recycling [3]. Nevertheless, there are limiting factors for the application of HSS grades: they usually show low formability with some difficulties like its low ductility, wrinkles and springback [4,5].

In view of this situation, industrial users focus on finding ways to obtain accurate predictions of the part geometrical features and post-forming characteristics. In addition, the prediction of possible defects and failures on the basis of the process parameters has also been studied [6]. In this context, numerical simulation by finite element method (FEM) is widely used as a tool for engineers to improve the part design taking into account the process limitations.

In forming operations, the metal sheets are normally subjected to bending-unbending and stretching processes, for example when a sheet is drawn over a die corner [7] or when it is subjected to a roll levelling process [8]. In these cases, the material is subjected to complex strain paths which make it difficult to accurately predict the final shape of the part after forming. For that reason, the accuracy and quality of the final product are highly dependent on the accuracy of the implemented material constitutive model amongst others.

Constitutive models can be defined by two different ways: by the physical theory (defined at microscopic level) and the phenomenological theory (defined at macroscopic level). Microstructural models for sheet metal forming simulations show a high accuracy level on the dislocation and phase transformation mechanics [9,10]. However they are currently limited in their use, especially in industry, due to the complex experimental techniques required for the identification of their material parameters [6] as well as the associated high computational cost.

On the other hand, the macroscopic models are widely used, since they provide good compromise between model accuracy and simulation computational time [11]. Complex models are introduced increasingly in FEM codes to provide accurate predictions of material behaviour and different phenomenon such as the Bauschinger Effect, the transient behaviour, the permanent softening and ratcheting. Predictions of all these phenomena which affect the final shape are linked to the hardening rule, which describes the evolution of the initial yield surface. In fact, various types of hardening models can be used, according to their ability to explain and predict the details of the plastic behaviour during a given deformation process. Eggertsen et al. [12] collected the cyclic phenomena that are captured by different hardening models. They determined that as the complexity of the model increased, the model was able to increase the accuracy of the predictions.

There are three types of hardening models: the isotropic models, the kinematic models and the combination of both. For simple applications, isotropic hardening models are used by

expressing the proportional expansion of the initial yield surface [13]. These models have been widely used for industrial applications due to their simplicity and because they are able to predict hardening behaviour of a high range of different materials. Nevertheless, the simulation of new advanced materials, such as AHSS, introduces a challenge as the use of isotropic models overestimates the hardening in reversal loading under reverse strain paths [6]. This is due to the presence of different phenomena during reversal loading which occur commonly in these materials, such as: the Baushinger effect, the transient behaviour and the permanent softening [14].

Kinematic hardening laws provide more sophisticated models than isotropic, where yield surfaces preserve their shape and size but translate through the stress space. In recent years these models have received special attention due to their ability to predict some phenomena such as the Bauschinger Effect [12,15]. This phenomena is a clear example of how the mechanical response of a metallic material depends not only on its current stress state but also on its deformation history. It describes the early re-yielding that occurs when reversing the load [16]. This is characterized by two stages which are presented in Fig. 1. Firstly, the transient Bauschinger deformation is composed of early re-yielding and smooth elastic-plastic transition with a rapid change of work hardening rate [17]. The second stage is the permanent softening defined by stress offset in a region after the transient period [18].

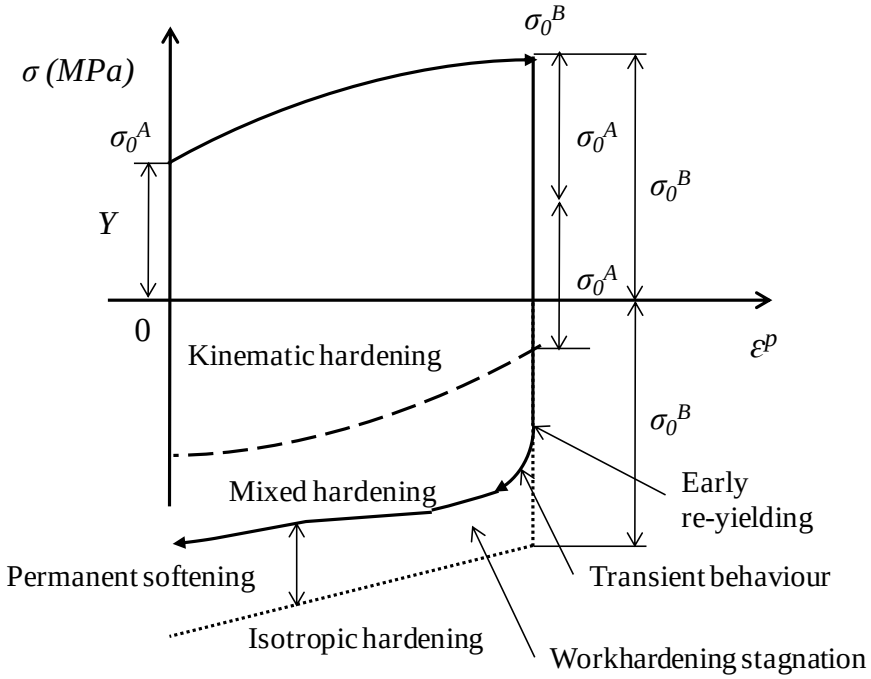

Figure 1: Bauschinger Effect description

A combination of the isotropic and a non linear kinematic hardening rule provides a uniform expansion and translation in shape of the yield surface. These types of mixed hardening models are proved to predict properly material behaviour of AHSS [19]. Kim et al. [10] found that the hardening behaviour including the Bauschinger and transient behaviour was well represented by a modified mixed Chaboche model for dual phase materials. Shi et al. [20] determined the constitutive parameters for a combined isotropic-kinematic hardening model based on the Yoshida Model for several AHSS, such as DP980 and DP780. The model was able to predict the stress and strain behaviours in various cycle tension and compression tests. Gil et al. [21]

proved that a mixed hardening model was able to predict much more accurately the final geometry of a component of DP1000 than a standard isotropic hardening model. Currently, the Chaboche and Lemaitre mixed hardening model (1990) [22] is one of the most widely accepted in sheet metal forming simulations due to its simplicity and it is being implemented in most of Finite Element Codes. The model is the result of the combination of both the Voce isotropic hardening law [23] and the Armstrong-Frederick nonlinear hardening law [24].

The accuracy and complexity of models depend on the number of material parameters and history variables. Each model has its precise requirements in terms of experimental data and testing needed to identify its parameters. For example, isotropic hardening models are identified on the basis of experimental data obtained from monotonic test methods, e.g. Mendiguren et al. [25] obtained the Ludwik hardening model parameters from tensile tests of a Ti64Al4V alloy and for a MS1200 steel. However, in the characterization of forming operations, cyclic loading experimental tests are usually used in order to analyse kinematic hardening [19]. Different authors have proposed several reverse loading tests. Experimental data using a tension-compression test were obtained for different dual phase materials by Grüber et al. [26], who used these parameters to simulate roll levelling process. This is a low deformation process in which bending/unbending loading are involved. Brunet et al. [27] identified the hardening parameters by using bending test of a mild steel, however the results showed some limitations and uncertainties due to the fact that the strain state in the sample was not exactly a pure strain state of bending. The cyclic three point bending test was also used to determine various hardening laws of DP600 and 220IF steels by Eggertsen and Mattiasson [28]. This test required an inverse approach which involves considerable computing time.

Other authors compared different tests, such as Carbonnière et al. [29], who compared bending and simple shear test on a TRIP steel and an aluminum alloy and enabled to achieve higher deformations. Eggertsen and Mattiason [12] also compared hardening parameters determined from bending test and those determined from tensile/compression tests for DP600 steel. In both cases, each experiment yields a different set of hardening parameters, however numerical simulations from both tests seemed to yield the same level of accuracy. Suttner and Merklein [30] identified the kinematic parameters of Chaboche and Rousselier by tension-compression tests and implemented them in a numerical model of shear test providing good results. In that case, the transferability of the identified kinematic hardening parameters to different stress states was possible.

Nevertheless, tension-compression tests are the most simple and straight-forward test [31]. This is because the stress-strain data are obtained directly during the course of the test and an inverse method is not necessary, as occurs in pure and three point bending test [32]. This test only achieves a maximum deformation of approximately 3%, however it could be appropriate to characterize low deformation processes such as roll levelling process, in which the maximum material deformation is usually lower than 2%. Nevertheless, the test is difficult to perform, due to the tendency of the specimen to buckle in compression [33].

Although all tests are suitable for simulating forming process, the modeling of the experimental curves obtained from different tests provide a set of parameters unique [34]. For example, Broggiato et al. [15] performed tension-compression tests at different strain amplitudes and three point bending test with three materials: DP600, TRIP700 and AISI316L. Different values of the material parameters for each case were obtained in the fitting of a non linear kinematic hardening model. For this reason, it is important to follow the same methodology to be able to

compare different materials parameters, i.e. to use the same experimental test, hardening law and parameter identification method.

The present study focuses on the analysis and modeling of hardening behaviour of a wide range of materials from mild steels up to advanced high strength steels. For this purpose, in the first part of the paper the response of materials when they are subjected to cyclic plastic deformation from a phenomenological point of view is studied. In particular, the Yield strength evolution, the Bauschinger Effect and the distribution of hardening (isotropic and kinematic) have been determined for a wide range of materials: from mild and stainless steels to Advanced High Strength Steels (AHSS).

In the second part of the paper the same methodology has been used to model the hardening behaviour of all these steel families. Specially, the characterization has been carried out by means of cyclic tension-compression tests at low strain ranges. The mixed Chaboche and Lemaitre hardening law was used to fit the experimental curves by means of a parameters optimization technique.

2. Material characterization procedure

2.1. Material properties

In order to develop numerical models to simulate a process, it is essential to analyse how materials behave when they are subjected to strain paths similar to the ones in forming processes. In particular, most sheet metal forming operations undergo cyclic deformations, e.g. drawing operations or levelling processes. In order to cover a wide strength range of materials, the characterization of different steel families subjected to these kinds of loadings was carried out. Material behaviours and evolution of their hardening properties with accumulated plastic strain was analysed. Monotonic tensile tests were performed on three samples at room temperature and one representative curve was taken. All the studied materials had 1.5 mm thickness and are presented in Table 1 together with their main averaged mechanical properties. The true stress strain curves from tensile tests can be found in Fig. 2.

Table 1: Material properties of studied materials

Material family	Material	Young's Modulus (GPa)	Yield strength (0.2% offset) (MPa)	Ultimate tensile strength (MPa)	Elongation (%)
Mild Steel	DC01	204.28	144.46	420.70	41.67
Stainless steel	430BA	178.35	238.31	513.12	28.30
	316L	168.36	327.45	1048.20	49.67
High Strength Steels	S420MC	199.13	440.73	623.47	20.69
Advanced High Strength Steels	TRIP700	209.22	495.90	961.41	29.69
	DP1000	202.39	922.19	1055.75	8.74
	MS1200	199.72	1238.10	1332.23	5.18

Mild steel DC01 shows the lower strength material with a ferritic microstructure. High Strength Low Alloy Steels (HSLA), such as S420MC, consists of ferrite and fine carbonitrides with yield

strengths from 210 to 550 MPa. These materials are designed to provide better mechanical properties than conventional carbon steel. They are hardened by a combination of precipitation and grain size refining, resulting in high strength with low alloy content [35].

Advanced High Strength Steels, such as TRIP700, DP1000 and MS1200 show greater yield strengths and tensile strengths. These materials are primarily multiphase steels, which contain ferrite, martensite, bainite, and/or retained austenite in quantities sufficient to produce desired mechanical properties [4]. Low-alloy transformation-induced plasticity (TRIP) steels consist of a ferrite matrix, containing bainite, martensite and a fraction of a metastable retained austenite. Under plastic deformation, the retained austenite transforms into martensite, which means these steels have a desirable combination of high strength and high ductility [5] as can be observed in Fig. 2. However AHSS materials containing higher amounts of martensite such as DP1000 and MS1200 show a limited formability. DP1000 consists on a soft ferrite matrix and a significant martensite second phase and MS1200 is characterized by a martensitic matrix containing small amounts of ferrite and/or bainite [36]. In general, the higher the yield strength of the material, the lower the ductility due to the increase of martensite content.

Stainless Steels are also presented in Fig. 2. These are interesting materials from a corrosion point of view, and they have adequate mechanical properties and manufacturing characteristics. 316L stainless steel belongs to the austenitic stainless steel family which undergoes strain-induced martensitic transformation due to plastic deformation. The strain-induced martensitic transformation may substantially enhance their formability by increasing the strain hardening rate, ductility and ultimate tensile strength [37]. 430BA is one of the widely used ferritic stainless steel grades with a high amount of chromium which provides a better corrosion resistance.

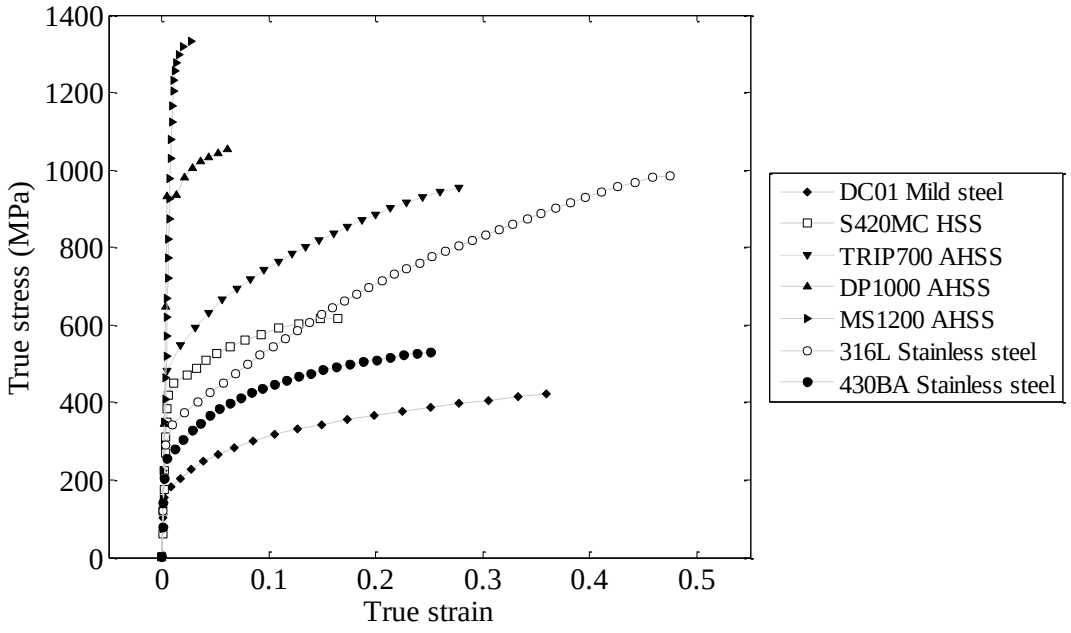

Figure 2: True tensile curves of different steel families

2.2. Experimental procedure

The tension-compression test proved to be an appropriate experimental test to characterize the Bauschinger Effect and the identification of the material parameters of the kinematic hardening laws [32]. The test provides suitable stress-strain curves under small strain ranges, however the maximum plastic strain achieved with this method is limited. Another inconvenience of this test is the buckling for thin sheet in compression loading. For this reason different authors have developed devices so as to avoid this effect. Kuwabara et al. [38] proposed a sheet specimen which is sandwiched between two pairs of male and female dies. Eggertsen and Mattiasson [32] developed similar equipment to prevent the buckling by applying a normal contact between the device and the specimen during testing. Yoshida et al. [39] suggested bonding five pieces ofsheets together before machining them so that the thickness of the specimen was 5.0 mm. Bae and Hug [33] used a spring-loaded clamping device in various strain rates. More recently, a transparent wedge device was designed to prevent the buckling of thin sheets, allowing full field strain measurements of the specimen using digital imaging methods [40]. In the present study, a special tool to avoid buckling was also developed and its description is presented below.

The specimens were cut using a wire EDM from sheet in the 0º rolling direction. They were rectangular with 1.5 x 12.5 mm^2 cross section and a gauge length of 22.5 mm. The geometry of the samples was specifically designed for this study, with the aim of using them in a tool to avoid buckling. Figure 3 shows the specimen geometry.

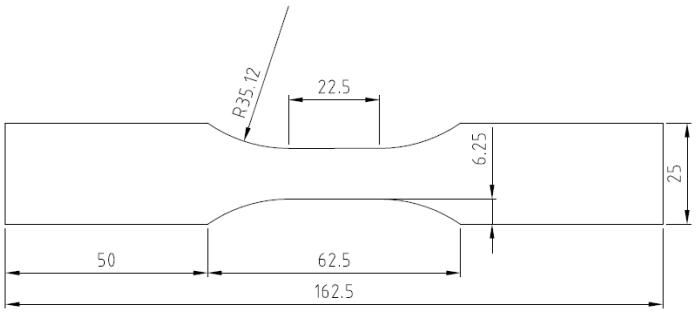

Figure 3: Specimen geometry for the tension-compression test

A servo hydraulic MTS 810 Material Test System was used for the experiments. Force data was acquired through an axial 100 kN load cell and strain data was measured with strain gages to obtain a continuous measurement. In particular, small deformation strain gages [41] were selected (strain range ±3%). It has been selected this measurement system due to its good precision and low size of the sensor (5.33x5.84 mm^2 matrix length x width). The strain gage was glued on the specimen in order to the position of the gage coincides with the hole of the upper die. In this way, the gage was not damaged. The wires passed through the hole of the upper die and were connected to the acquisition systems.

Figure 4 shows the experimental test equipment used with the tool to avoid buckling during the test. The specimen was clamped between the two holders leaving a 0.1 mm gap and was lubricated by Rhenus Fe 1300 high viscosity lubricant to eliminate the influence of friction during the test [25].

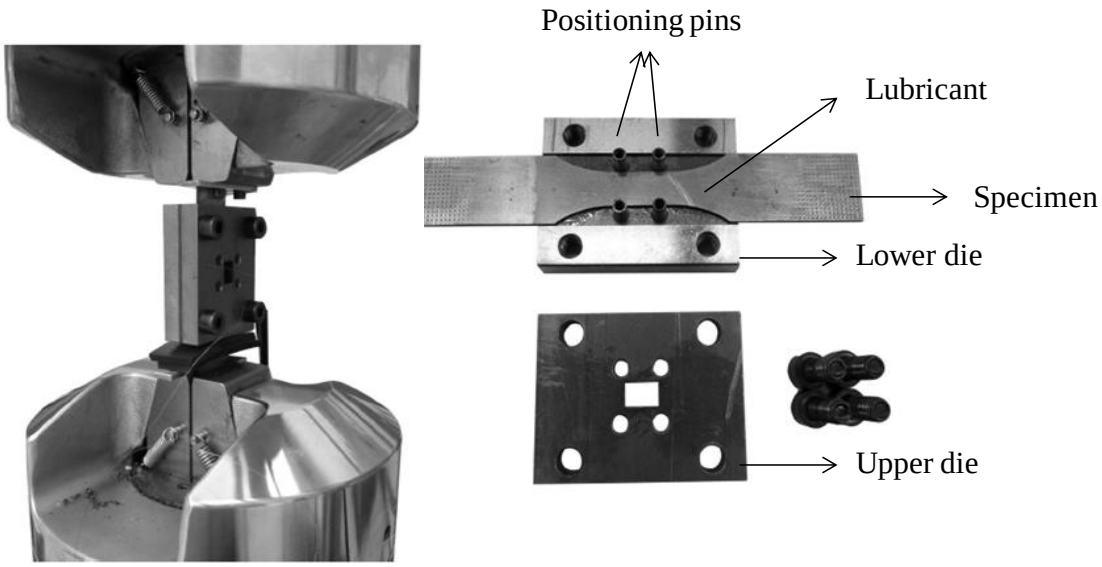

Figure 4: Experimental test equipment

The test started from a relaxed configuration, then the specimen was stressed in traction until 2% deformation at a rate of 0.03 mm/s. In this point the load was reversed, and the sheet was discharged until a relaxed level of stress. Next, the specimen was loaded in compression until -2%. Once the maximum compression strain was achieved, the load was reversed again for discharging the accumulated stress in the specimen, closing the cyclic curve. This process was repeated for three cycles. The maximum deformation which can be achieved by this test is limited by bucking in compression. For this reason the amplitude of the cycles during the test was ±2%.

3. Cyclic Hardening Analysis

Hardening analysis is related to the study of the evolution of the yield strength when the accumulated plastic strain increases and other characteristic phenomena of cyclic plasticity such as the Bauschinger Effect. It provides information about the hardening behaviour of the different steel families to be subsequently modelled with an appropriate hardening law.

The analysis requires the experimental stress-strain curves from the tension-compression test. Figure 5, 6, 7 and 8 show the experimental curves of the different steel families previously reviewed. A tendency to reduce the cyclic hardening as the yield strength of the materials increase is shown. For example, DC01 mild steel exhibited a pronounced cyclic hardening (Fig. 5), while AHSS tended to reduce this effect. This reduction is even more pronounced in DP1000 and MS1200 which show a cyclic softening. In addition, the Bauschinger Effect seems to be more pronounced for high yield strength materials. The increase of the Bauschinger Effect is reported to be related to the increase of a harder second-phase martensite in the ferritic matrix [42]. Regarding Stainless Steels, both materials had a marked cyclic hardening, but 316L stainless steel had a progressive saturation of its hysteresis loops and a fast saturation of the hysteresis loops was observed in 430 BA stainless steel.

- *Mild Steel*

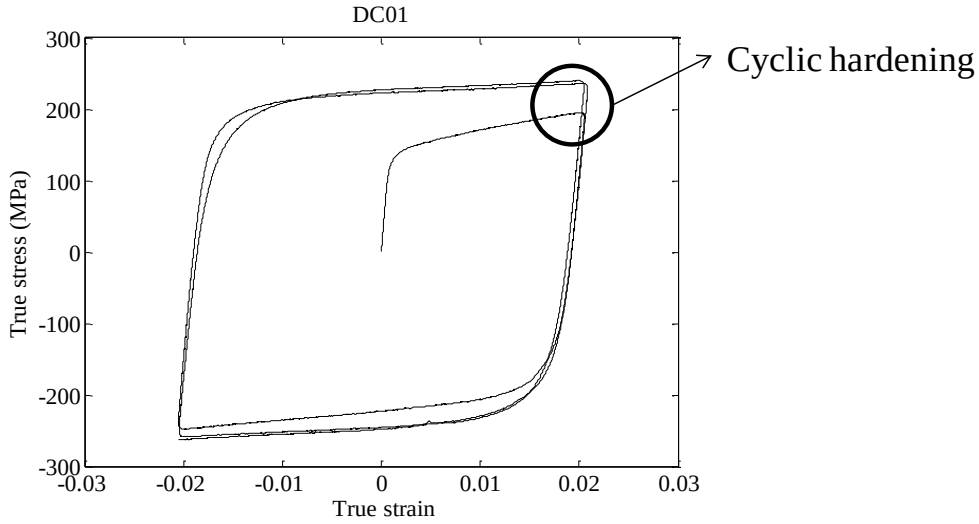

Figure 5: Tension-compression experimental curve of DC01 Mild Steel

- *High Strength Steel*

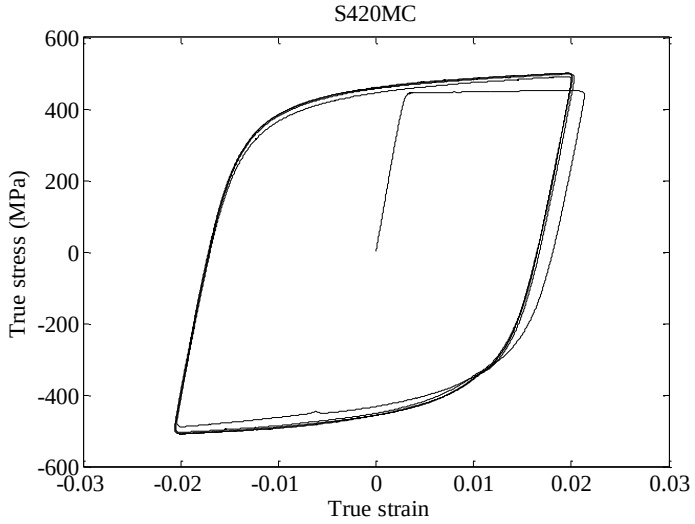

Figure 6: Tension-compression experimental curve of S420MC HSS

- *Advanced High Strength Steels*

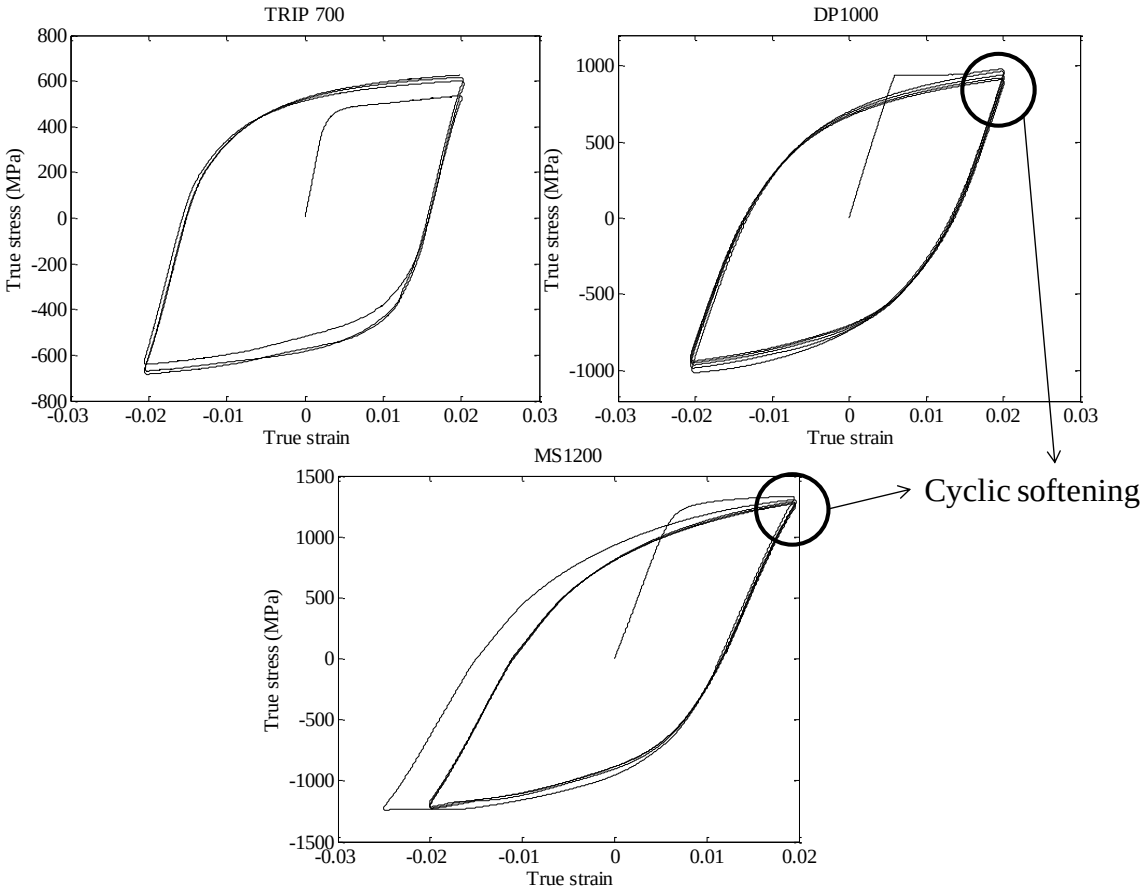

Figure 7: Tension-compression experimental curve of TRIP700, DP1000 and MS1200 AHSS.

- *Stainless steel*

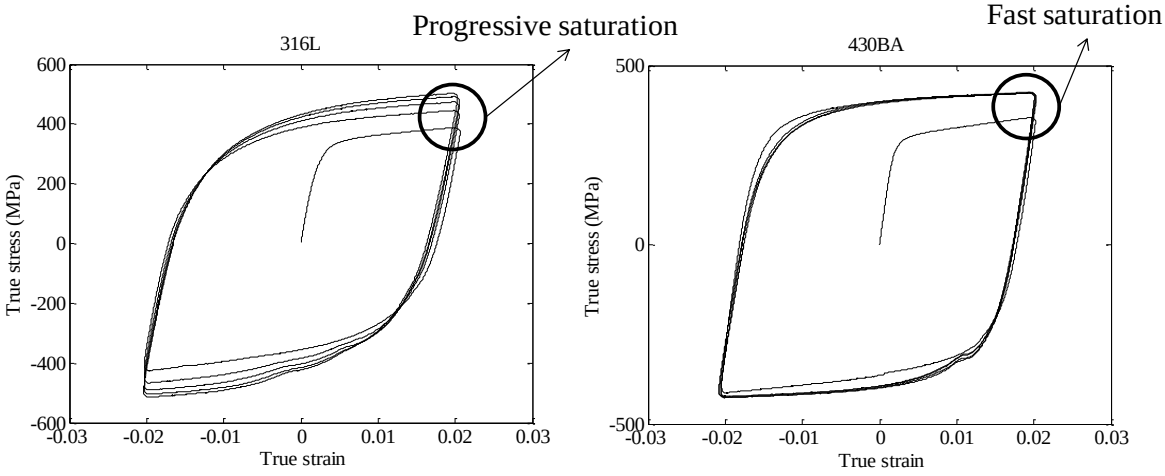

Figure 8: Stainless Steel cyclic loading experimental curves.

Yield Strength evolution

The evolution of the Yield strength with accumulated plastic strain was analysed. In order to compare these values the normalized Yield strength in each cycle, in loading and unloading

paths, was calculated as the ratio between the Yield strength in each cycle and the initial Yield strength. The values are represented for the different materials in Fig. 9.

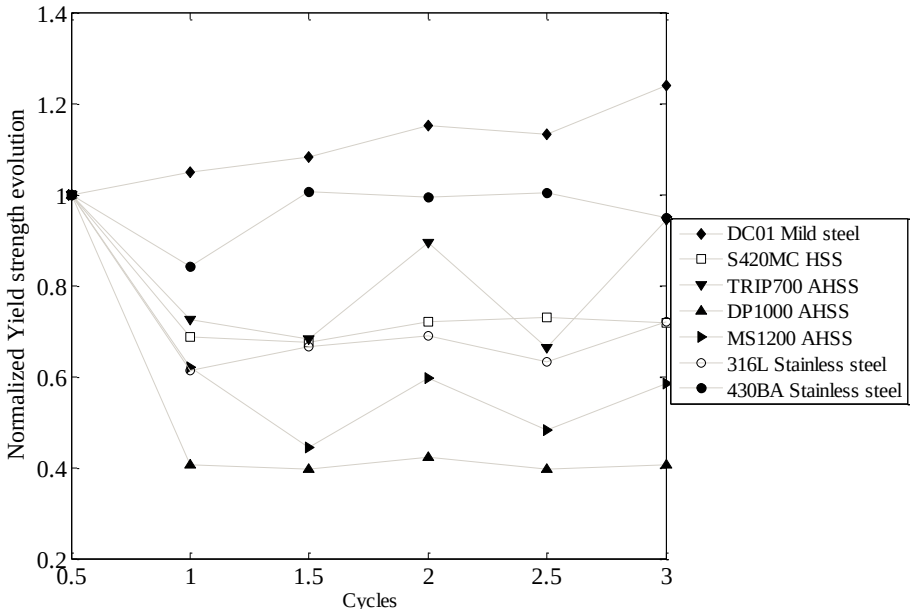

Figure 9: Normalized Yield strength evolution for different steel grades

With the exception of DC01 (which showed an increase at each cycle in yield strength) and 430BA Stainless Steel (which provided relatively stable yield strength values) most materials showed a pronounced initial reduction in yield strength. This initial reduction can be attributed to the Bauschinger effect.

Yield strength evolution in the successive cycles could be related to the tendency of the material to saturate or not. DC01 is a clear example of a non-saturated material since its yield strength increased continuously. In contrast, the rest of the materials showed a constant yield strength value, which is indicative of saturated behaviour. Such behaviour suggests a stable microstructure of the material when it is subject to low cyclic deformation.

The Bauschinger Effect

The Bauschinger Effect seemed to be more significant as the yield strength of the material increased. In order to quantify this tendency, the degree of the Bauchinger effect was evaluated for each material by means of the Bauschinger ratio which was defined by Kim et al. [43]. In Fig. 10 the Bauschinger phenomenon is schematically represented. In this figure, the compressive behaviour is reversed in order to analyse the early re-yielding (Bauschinger Effect) and rapid change of the work hardening rate (transient behaviour). This technique has been widely applied by previous authors to represent the Basuchinger phenomena [18,44].

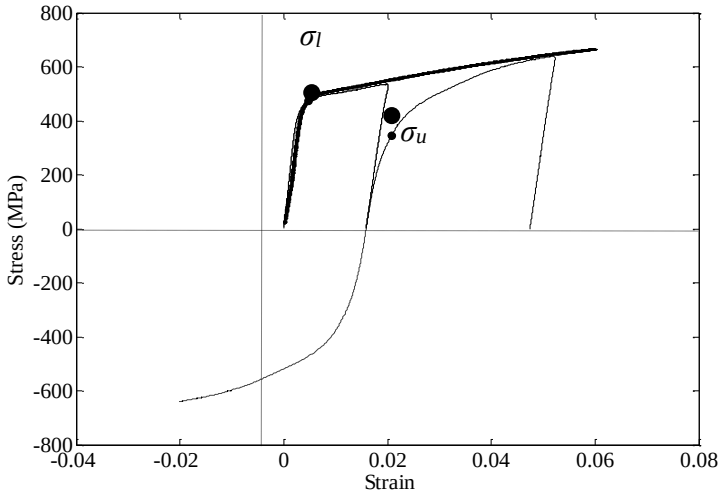

Figure 10: Bauschinger Effect analysis

The Bauschinger ratio (B.R.) is defined as,

$$B.R. = \frac{\sigma_l - \sigma_u}{2 \cdot \sigma_l}, \quad (1)$$

where σ_l is the yield strength at the start of loading and σ_u is the yield strength during the unloading. The Bauschinger Ratios (B.R.) for the studied materials are presented in Table 2. All the measurements of the yield point in the loading and unloading were determined by the 0.2% offset method. Most of materials were found to be influenced by the Bauschinger Effect (B.R. <=1). The smaller the B.R. is, the larger the Bauschinger Effect becomes. For isotropic behaviour materials, which are hardly ever affected by Bauschinger Effect, the B.R. tends to 1.

Table 2: Bauschinger ratio of different steel families

Material	DC01	S420MC	TRIP700	DP1000	MS1200	316L	430BA
B.R.	1,025	0.843	0,863	0,703	0,806	0,810	0,921

DP1000, which presents the lower B.R., shows to be the material most influenced by this phenomenon. On the other hand, the DC01 shows a B.R. slightly higher than 1 due to the increase of yield strength during the unloading. These opposite behaviours can be attributed to a predominant isotropic behaviour of the material in the case of DC01, and a relevant kinematic behaviour in the case of DP1000. Regarding Stainless Steels, similar tendencies in their behaviours have been noticed. Austenitic 316L stainless steel shows a considerable Bauschinger Effect (B.R.=0.810), while ferritic 430 BA stainless steel tends toward an isotropic behaviour (B.R.=0.92).

In light of these results, it can be concluded that the cyclic behaviour and the scale of the Bauschinger Effect is related to the microstructure composition. Ferritic materials show a tendency toward isotropic behaviour and they are not significantly affected by the Baushinger phenomena. On the other hand, the existence of several phases with different strengths, such as the combination of martensite, austenite and ferrite, suggests a variation in the strain mechanism of the material which causes the occurrence of the Bauschinger effect and therefore, the kinematic behaviour.

Isotropic and kinematic hardening evolution

Previous authors have concluded [15,45,46] that the real behaviour of metals falls between both models: Isotropic and Kinematic. In the previous section, it was observed that the yield strength changes with the accumulated plastic strain. This evolution of the yield strength, and therefore, the hardening of the material can be associated with an isotropic hardening, a kinematic hardening or both. In general, it has been found that as the initial yield strength of a material increases, its hardening response tends toward a kinematic behaviour, while the low yield strength materials tend toward an isotropic behaviour [31].

In this section the evolution of isotropic hardening and kinematic hardening were studied for each material with the aim of determining the distribution of hardening in different materials. The isotropic hardening was calculated by means of the isotropic variable R_1:

$$R_1 = \frac{(\sigma_C - \sigma_B) - 2 \cdot \sigma_A}{2}, \tag{2}$$

and the kinematic hardening was calculated by means of the displacement of the backstress X_1:

$$X_1 = \frac{\sigma_C - \sigma_B}{2}. \tag{3}$$

The definition of the reference stresses, $\sigma_A, \sigma_B, \sigma_C$ is schematically presented in Fig. 11 where a characteristic strain path reversal is shown.

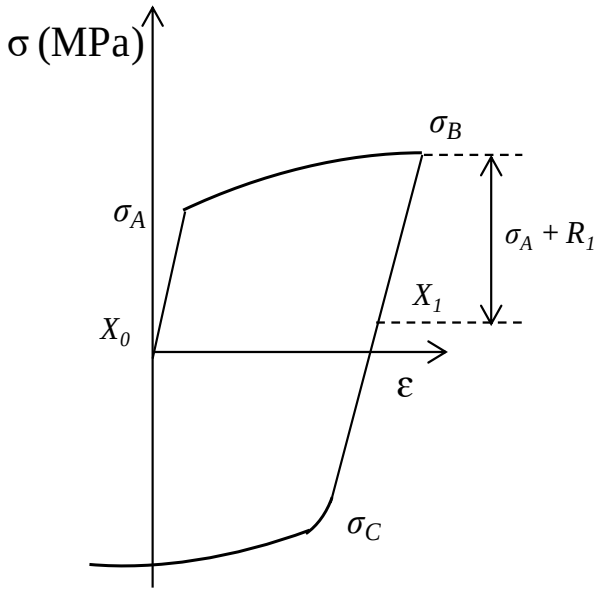

Figure 11: Schematic representation of isotropic and kinematic hardening

The isotropic parameter *R* and the backstress *X* were calculated in each load and unload for several cycles. The evolution of *R* and *X* when the accumulated plastic strain increased is presented in Fig. 12 and 13 respectively for all the materials. The representation of the variables was normalized to the yield strength (R/σ_0 and X/σ_0) in order to be comparable to each other. In addition, a trend line was fitted to the experimental points in order to show the trend of the hardening.

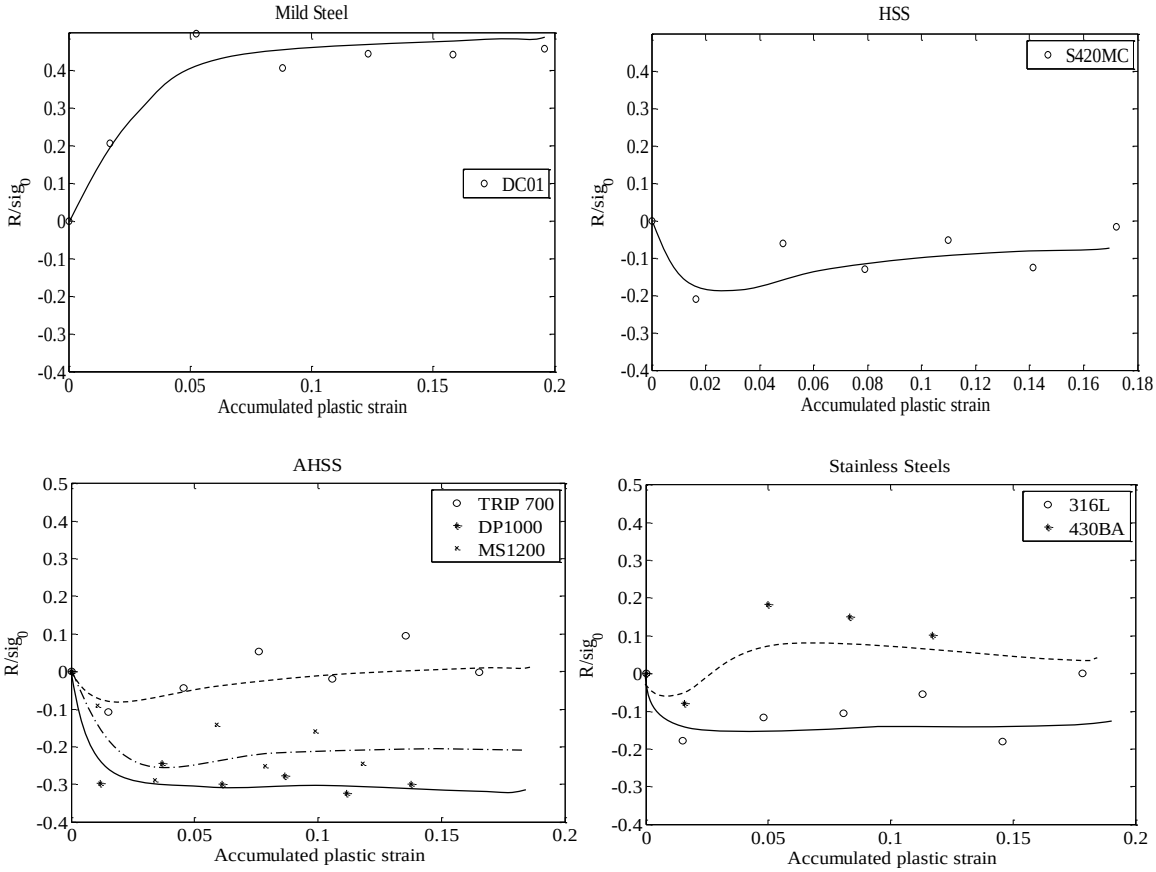

Figure 12: Evolution of isotropic hardening parameter R

Regarding the evolution of isotropic hardening, two clear behaviours can be detected in Fig. 12. Materials with lower yield strength, such as the DC01, show a trend to increase the value of the isotropic parameter *R*. This means that yield surface is expanding with accumulated plastic strain. The opposite behaviour takes place for materials with high yield strength, such as DP1000 and MS1200. The trend of these materials is to reduce the value of the isotropic hardening, that is to say, its yield surface is reduced with accumulated plastic strain. Materials with intermediate values of yield Strength show an oscillating value around cero. In all cases, the evolution of the isotropic hardening seems to suggest a saturated behaviour, which could be predicted by the Voce type hardening law [13].

The Backstress parameter was represented in absolute value (Fig. 13). In general, a pronounced increase of the backstress was observed in all the materials in the first load, followed by a stabilization of its value in the remaining cycles.

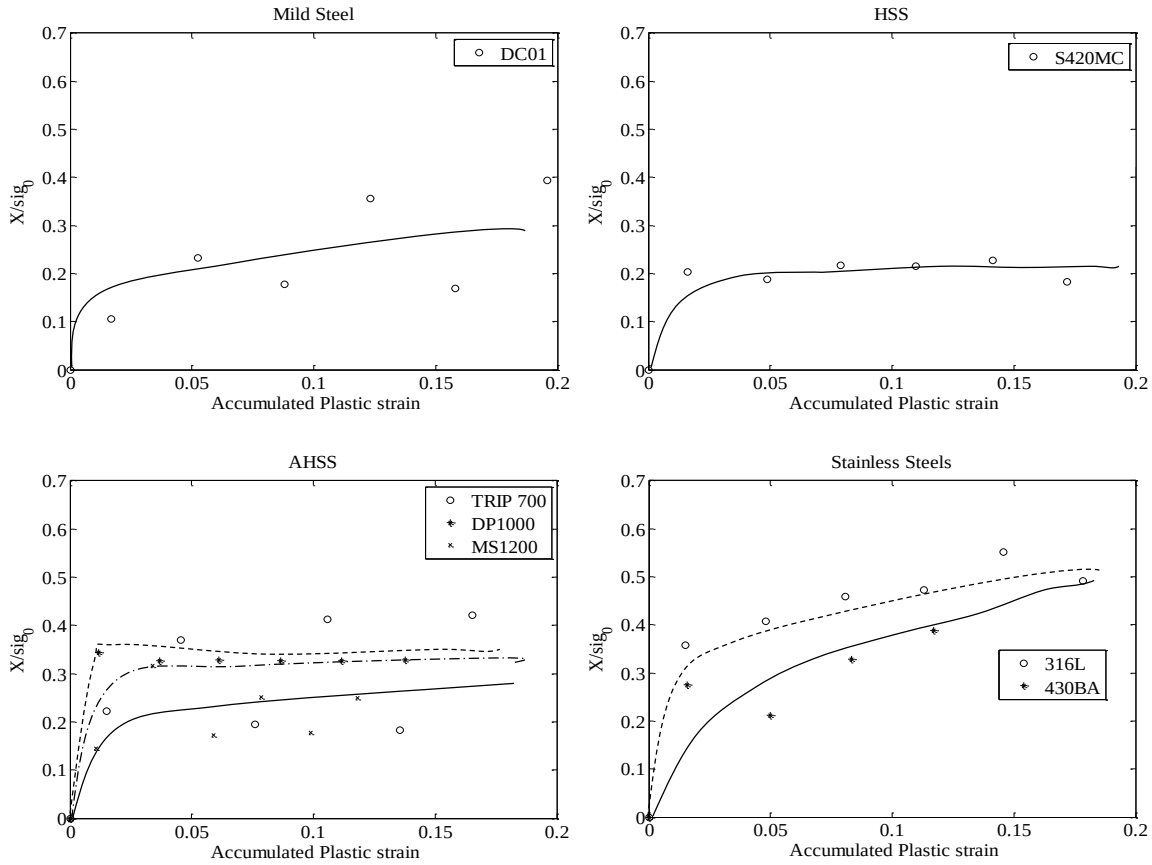

Figure 13: Evolution of backstress X

4. Parameter identification of mixed Chaboche and Lemaitre hardening model

The purpose of this section is to collect a set of hardening parameters of a wide range of materials obtained by the same method, with the aim of providing comparable values. The experimental data from the tension-compression tests were used as target curves in the optimization procedure. Then, the material parameters involved in the mixed isotropic-kinematic Chaboche and Lemaitre model with one backstress were fitted to the experimental curves [15,47].

Mixed isotropic-kinematic hardening model of Chaboche and Lemaitre (1990)

The Chaboche and Lemaitre hardening model (1990) [22] was applied with Von Mises yield criteria, as these are recommended for cyclic plasticity analyses and widely distributed in commercial FE-codes [46]. The Von Mises yield criteria can be expressed:

$$\phi(\boldsymbol{\sigma}, \boldsymbol{X}, \sigma_y) = \sqrt{\frac{3}{2}(\boldsymbol{\sigma} - \boldsymbol{X}) : (\boldsymbol{\sigma} - \boldsymbol{X})} - \sigma_y - R, \tag{4}$$

where $\boldsymbol{\sigma}$ denotes the deviatoric stress tensor, X is the deviatoric backstress tensor, σ_y is the initial yield stress and R is the isotropic hardening. Considering an associated flow rule, the plastic strain increment is defined as:

$$\mathrm{d}\boldsymbol{\varepsilon}^p = \mathrm{d}\lambda \cdot \frac{\partial \phi}{\partial \boldsymbol{\sigma}}, \tag{5}$$

where $\mathrm{d}\boldsymbol{\varepsilon}^p$ is the plastic strain rate and λ represents the plastic multiplier, which is defined as non negative, and must satisfy the consistency condition $\phi \cdot \lambda = 0$. The Chaboche and Lemaitre hardening model is a mixed isotropic-kinematic hardening formulation. The nonlinear kinematic hardening describes the movement of the yield surface by means of the evolution of the backstress. The change in the size of the yield surface, is related to the isotropic hardening and is introduced by means of the initial value of the yield strength σ_y and the isotropic variable R.

In the proposed model, the evolution of isotropic hardening is defined in function of the accumulated plastic strain $\mathrm{d}\bar{\varepsilon}^p$ by the following law:

$$\mathrm{d}R = b \cdot (Q - R) \cdot \mathrm{d}\bar{\varepsilon}^p, \tag{6}$$

where Q and b are material parameters of the model. The accumulated plastic strain on the other hand is defined as:

$$\bar{\varepsilon}^p = \int_0^t \dot{\varepsilon}^p \cdot \mathrm{d}t\,. \tag{7}$$

The kinematic evolution of the yield surface, proposed by Chaboche et al. [48], is presented in Eq. (8). This model is based on a decomposition of the non-linear kinematic hardening rule proposed by Armstrong and Frederik (1966). Chaboche decomposed a stable hysteresis curve in several parts, and it was observed that increasing the material parameters of the hardening rule by the superposition of backstresses, a more accurate model was obtained [49,50]. However, in this work only one backstress has been considered in the model definition because of many FE codes have only implemented the model with one backstress.

$$d\boldsymbol{X} = {}^2\!/_3 \cdot C \cdot d\boldsymbol{\varepsilon}^p - \gamma \boldsymbol{X} \cdot \mathrm{d}\bar{\varepsilon}^p\,. \tag{8}$$

Therefore, the hardening parameters to identify from this model are two isotropic parameters: *b* and *Q*; and two kinematic parameters: *C* and *γ*.

Hardening parameter identification method and results

The parameter identification method consists of an unconstrained nonlinear optimization proposed by Nelder and Mead [51], so that the objective function is minimized. This objective function is defined as the difference between the predicted stress values by the model and the experimental data as is shown in the Eq.(9).

$$f_{obj} = \frac{1}{n}\sum_{i=1}^{n}\left|\frac{(\sigma_i^{exp} - \sigma_i^{model})\cdot 100}{\sigma_i^{exp}}\right| \tag{9}$$

The results of the fitting of the curves are presented in Fig. 14, 15, 16 and 17. As can be observed, the model was able to accurately predict the cyclic hardening and the cyclic saturation of the DC01 material. The fitting of this model with AHSS also predicted the Bauschinger Effect and the cyclic softening. However, the model was not able to predict accurately the transient behaviour.

- *Mild Steel*

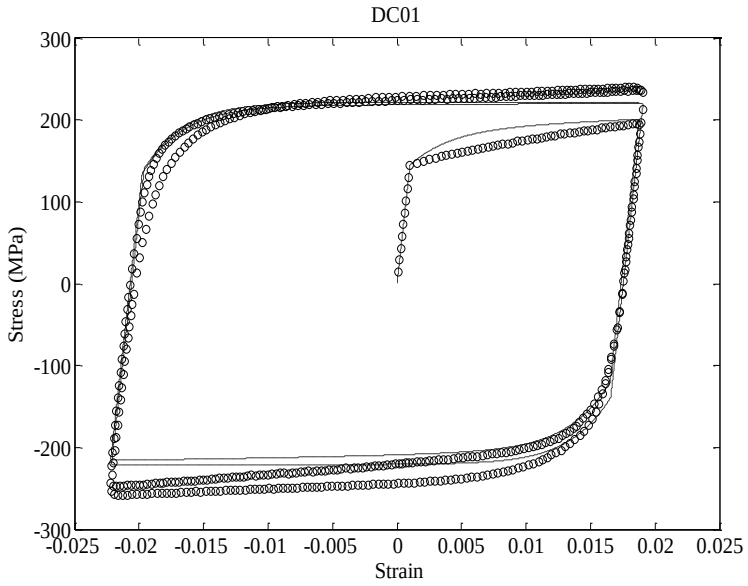

Figure 14: Fitting of Chaboche and Lemaitre model to experimental curve of DC01 Mild Steel

- *High Strength Steel*

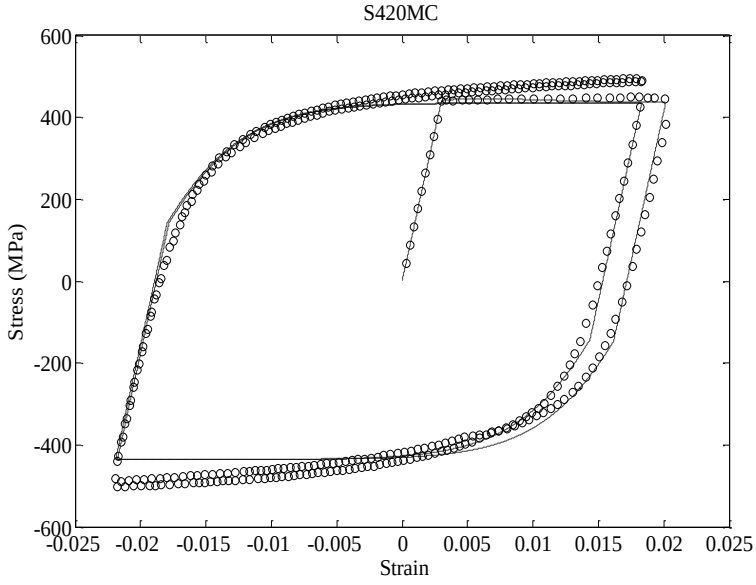

Figure 15: Fitting of Chaboche and Lemaitre model to experimental curve of S420MC HSS

- *Advanced High Strength Steels*

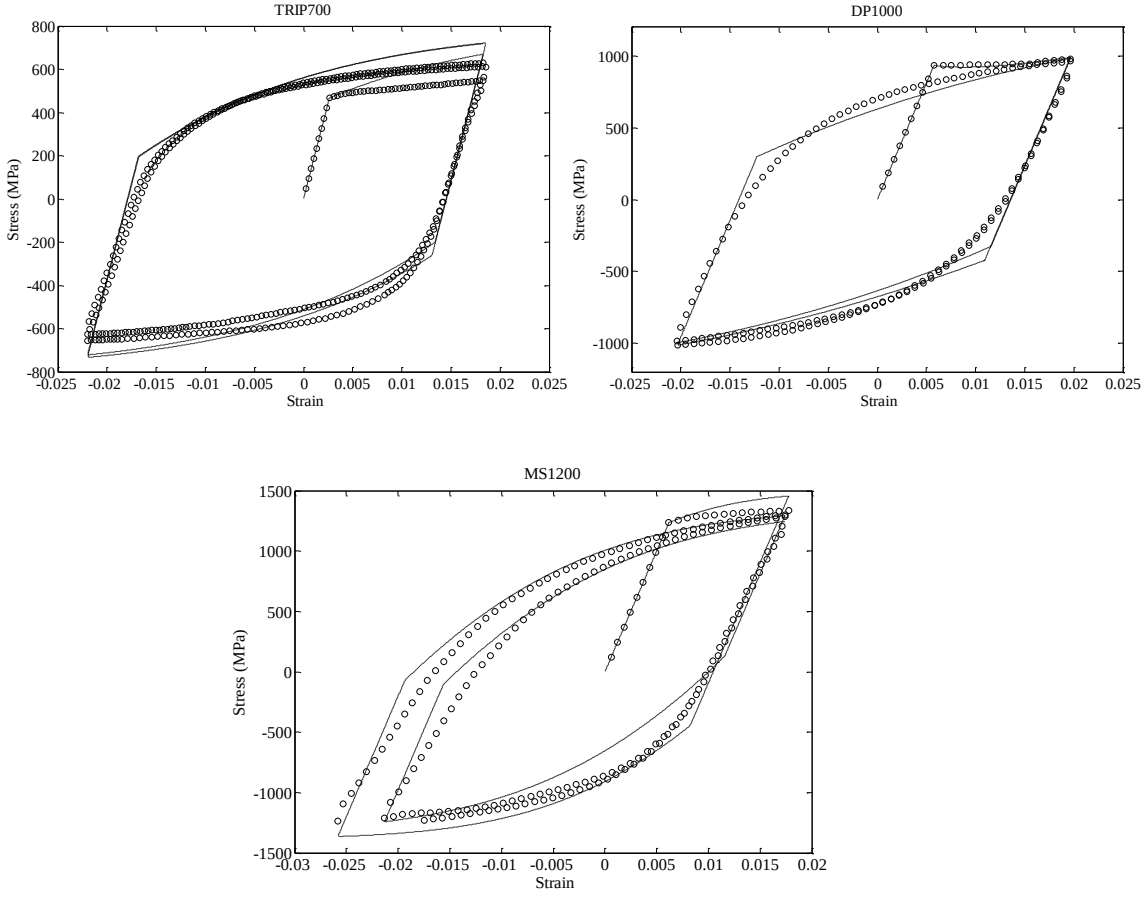

Figure 16:Fitting of Chaboche and Lemaitre model to experimental curve of TRIP700, DP1000 and MS1200 AHSS

- *Stainless steel*

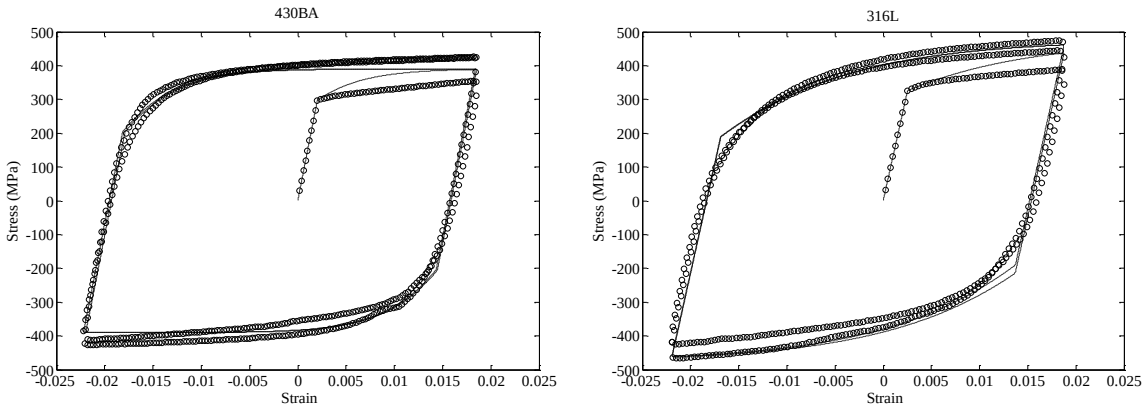

Figure 17: Fitting of Chaboche and Lemaitre model to experimental curve of 430BA and 316L Stainless Steels

The four material parameters involved in the model obtained by means of the same optimization method are presented for all the studied materials in Table 3. It can be observed that the positive or negative value of the isotropic parameter Q is related to the evolution of the

yield strength. In all the materials except DC01, the tendency of the yield strengths with regard their initial values was to reduce, which could be related to the negative value of Q. On the other hand DC01, which increased each cycle its yield strength, showed a positive value of this parameter.

Kinematic parameters are related to the hardening slope. In general, the higher the value of parameter C and the lower the value of the parameter γ, more pronounced the hardening slope is.

Table 3: Material parameters of the mixed Chaboche and Lemaitre hardening model

Material	Isotropic parameters		Kinematic parameters	
	Q(MPa)	b	C (MPa)	γ
DC01	36.89	32.20	144.46	363.63
S420MC	-151.28	239.64	40671.67	278.34
TRIP700	-22.64	3.7891	21425.40	62.7258
DP1000	-280.16	124.73	26276.72	34.88
MS1200	-670.31	53.05	76853.62	96.6717
316L	-96.05	277.69	36461.21	228.98
430BA	0.01	6.46	22807.60	243.32

5. Conclusions

The research outlined in this paper suggests that the types of materials employed in automobile manufacture depend more on material innovations rather than on manufacturing innovations. Therefore it is important to understand the material behaviour of new materials so as to adapt manufacturing process to their characteristics. Material characterisation by means of the tension-compression test proved to be a fast and easy test to recover cyclic reverse loading data. It revealed the different behaviours and different phenomena which take place during cyclic plasticity in a range of steel grades (mild steel, stainless steel and advanced high strength steels) as follows:

- During reverse deformation, the Bauschinger Effect was more pronounced in multiphase materials which show a significant strength difference between their phases, such as AHSS and Austenitic Stainless Steel.
- The evolution of cyclic hardening was also found to be related to yield strength, and therefore, to the microstructure composition. Ferritic materials which show low yield strength tend to reduce the cyclic hardening. While high yield strength materials which are composed by a combination of soft and hard phases, exhibited a cyclic softening.

Both conclusions confirm the association between the increase of hard-martensite phase in the microstructure of the material and its departure from isotropic hardening following stress reversals. The results are in agreement with recent studies [34,52].

With the regards to hardening modeling, the results revealed the importance of the isotropic hardening to model the behaviour of low yield strength steels, while high strength steels seem to be more influenced by kinematic hardening. However, for a proper description of hardening the behaviour, both Isotropic and Kinematic hardening are necessary. These results corroborate the ideas of Gil. et al. [21] and Suttner and Merklein [30], who suggested that a mixed hardening model was able to predict more accurately than a standard isotropic hardening model. Some correlations were found between the hardening behaviour of the material and the value of the parameters using the mixed Chaboche and Lemaitre model.

Acknowledgments

The work presented in this paper has been carried out in cooperation with FAGOR ARRASATE S. Coop. for its application in novel levelling machine design optimization. The authors are also grateful to the Spanish Science and Innovation Minister who financially support this work, through the INNPACTO National Program for Public-Private Cooperation.

References

[1] Willem Van der Wiel, J., Future of automotive design and materials, 2013 (2012).

[2] D Banabic, Sheet metal forming processes: constitutive modelling and numerical simulation, 1st ed., Springer, Heidelberg, 2010.

[3] WorldAutoSteel, Future Steel Vehicle, 2013 (2013).

[4] J Galan, L Samek, P Verleysen, K Verbeken, Y Houbaert. Advanced high strength steels for automotive industry, Revista de metalurgia. 48 (2012) 118-131.

[5] R Perez, J Benito, J Prado. Study of the inelastic response of TRIP steels after plastic deformation, ISIJ Int. 45 (2005) 1925-1933.

[6] S Bruschi, T Altan, D Banabic, P Bariani, A Brosius, J Cao, et al. Testing and modelling of material behaviour and formability in sheet metal forming, CIRP Annals-Manufacturing Technology. (2014).

[7] F Yoshida, T Uemori. A model of large-strain cyclic plasticity describing the Bauschinger effect and workhardening stagnation, Int.J.Plast. 18 (2002) 661-686.

[8] E Silvestre, J Mendiguren, E Sáenz de Argandoña, L Galdos, Roll levelling numerical simulation using a no nlinear mixed hardening material model, in: Wiley-VCH Verlag GmbH & Co. KGaA (Ed.), Steel research international, 2012, pp. 1295.

[9] B Peeters, SR Kalidindi, C Teodosiu, PV Houtte, E Aernoudt. A theoretical investigation of the influence of dislocation sheets on evolution of yield surfaces in single-phase BCC polycrystals, J.Mech.Phys.Solids. 50 (2002) 783-807.

[10] JH Kim, D Kim, F Barlat, M Lee. Crystal plasticity approach for predicting the Bauschinger effect in dual-phase steels, Materials Science and Engineering: A. 539 (2012) 259-270.

[11] B Haddag, T Balan, F Abed-Meraim. Investigation of advanced strain-path dependent material models for sheet metal forming simulations, Int.J.Plast. 23 (2007) 951-979.

[12] P- Eggertsen, K Mattiasson. On constitutive modeling for springback analysis, Int.J.Mech.Sci. 52 (2010) 804-818.

[13] S Bouvier, JL Alves, MC Oliveira, LF Menezes. Modelling of anisotropic work-hardening behaviour of metallic materials subjected to strain-path changes, Computational Materials Science. 32 (2005) 301-315.

[14] R Halama, J Sedlák, M Sofer, Phenomenological Modelling of Cyclic Plasticity, (2012).

[15] GB Broggiato, F Campana, L Cortese. The Chaboche nonlinear kinematic hardening model: calibration methodology and validation, Meccanica. 43 (2008) 115-124.

[16] Y Xiang, J Vlassak. Bauschinger effect in thin metal films, Scr.Mater. 53 (2005) 177-182.

[17] W Kubli, M Krasovskyy, M Sester. Modeling of reverse loading effects including workhardening stagnation and early re-plastification, nternational Journal of Material Forming. 1 (2008) 145.

[18] X Lemoine, A Aouafi. Bauschinger effect correspondence of experimental tests, International Journal of Material Forming. 1 (2008) 241-244.

[19] X Lemoine, L Durrenberger, H Zhu, R Kergen, Mixed hardening models: parameters identification on AHSS steels, Arcelor Mittal R&D.

[20] M Shi, X Zhu, C Xia, T Stoughton, Determination of nonlinear isotropic/kinematic hardening constitutive parameters for AHSS using tension and compression tests, (2008) 137-142.

[21] I Gil, L Galdos, U Ulibarri, E Sáenz de Argandoña, R Ortubay, E Silvestre, Influence of material's hardening law in the simulation of DP1000 deep drawing and subsequent springback , IDDRG Conference 2014. (2014).

[22] J Lemaitre, JL Chaboche, Mechanics of solid materials, Cambridge Univ Pr 1994.

[23] JL Chaboche. A review of some plasticity and viscoplasticity constitutive theories, Int.J.Plast. 24 (2008) 1642-1693.

[24] P Armstrong, Frederick CO, A mathematical representation of the multiaxial bauschinger effect, (1966).

[25] J Mendiguren, L Galdos, ES de Argandoña, E Silvestre. Ludwik's Model Parameter Identification for V-Bending Simulations with Ti64 and MS1200, Key Eng Mat. 504 (2012) 889-894.

[26] M Grüber, M Oligshläger, G Hirt. The effect of the initial stress and strain state in sheet metals on the roller levelling process, Key Engineering Materials. 651-653 (2015) 1023.

[27] M Brunet. Nonlinear kinematic hardening identification for anisotropic sheet metals with bending-unbending tests, Trans.ASME, J.Eng.Mater.Technol. 123 (2001) 378-383.

[28] P Eggertsen, K Mattiasson. An efficient inverse approach for material hardening parameter identification from a three-point bending test, Engineering with Computers. 26 (2010) 159-170.

[29] J Carbonnière, S Thuillier, F Sabourin, M Brunet, PY Manach. Comparison of the work hardening of metallic sheets in bending–unbending and simple shear, Int.J.Mech.Sci. 51 (2009) 122-130.

[30] S Suttner, M Merklein. Characterization of the bauschinger effect and identification of the kinematic chaboche model by tension-compression tests and cyclic shear tests, IDDRG Conference Proceedings- Innovations for the sheet metal industry. (2014) 125.

[31] E Silvestre, Sheet metal roll levelling process optimization by means of advanced models, (2013).

[32] P Eggertsen, K Mattiasson. On the identification of kinematic hardening material parameters for accurate springback predictions, International Journal of Material Forming. 4 (2011) 103-120.

[33] GH Bae, H Huh. Cyclic tension/compression test of auto-body steel sheets with the variation of the strain rate, IDDRG Conference. (2011).

[34] E Silvestre, J Mendiguren, L Galdos, E Sáenz de Argandoña. Numerical simulation of the roll levelling of DP1000 steel using a nonlinear combined hardening material model, Computer methods in material science. 15 (2015) 44.

[35] FB Pickering, High Strength Low Alloy Steels, Materials Science and Technology, Wiley-VCH Verlag GmbH & Co. KGaA, 2006,.

[36] S Keeler, M Kimchi, Advanced High Strength Steel (AHHS). Application guidelines, WorldAutoSteel. (2009).

[37] J Talonen, H Hänninen, P Nenonen, G Pape. Effect of strain rate on the strain-induced γ→ α′-martensite transformation and mechanical properties of austenitic stainless steels, Metallurgical and Materials Transactions A. 36 (2005) 421-432.

[38] T Kuwabara, Y Morita, Y Miyashita, S Takahashi. Elastic-plastic behavior of sheet metal subjected to in-plane reverse loading, Journal-Japan soociety for technology plasticity. 36 (1995) 768.

[39] F Yoshida, T Uemori. A model of large-strain cyclic plasticity describing the Bauschinger effect and workhardening stagnation, Int.J.Plast. 18 (2002) 661-686.

[40] J Magargee, J Cao, R Zhou, M McHugh, D Brink, F Morestin. Characterization of tensile and compressive behavior of microscale sheet metals using a transparent microwedge device, Journal of Manufacturing Science and Engineering. 133 (2011) 064501.

[41] Vishay Micro-measurements, General purpose strain gages - linear pattern, (2015).

[42] L Zhonghua, G Haicheng. Bauschinger effect and residual phase stresses in two ductile-phase steels: Part I. The influence of phase stresses on the Bauschinger effect, Metallurgical Transactions A. 21 (1990) 717-724.

[43] D Kim, M Lee, C Kim, ML Wenner, RH Wagoner, F Barlat, et al. Measurements of anisotropic yielding, Bauschinger and transient behavior of automotive dual-phase steel sheets, Metals and Materials International. 9 (2003) 561-570.

[44] M Lorenzo, B González, J Matos, L Aguado, V Kharin, J Toribio. Análisis del efecto Baushicnger en aceros de alta resistencia, Anales de Mecánica de la Fractura 26. 1 (2009).

[45] MC Araujo, Non-linear kinematic hardening model for multiaxial cyclic lasticity, (2002).

[46] L Jia, H Kuwamura. Prediction of Cyclic Behaviors of Mild Steel at Large Plastic Strain Using Coupon Test Results, J.Struct.Eng. 140 (2014) 04013056.

[47] B Chaparro, S Thuillier, L Menezes, P Manach, J Fernandes. Material parameters identification: Gradient-based, genetic and hybrid optimization algorithms, Computational Materials Science. 44 (2008) 339-346.

[48] JL Chaboche. Constitutive equations for cyclic plasticity and cyclic viscoplasticity, Int.J.Plast. 5 (1989) 247-302.

[49] S Bari, T Hassan. Anatomy of coupled constitutive models for ratcheting simulation, Int.J.Plast. 16 (2000) 381-409.

[50] A Mahmoudi, S Pezeshki-Najafabadi, H Badnava. Parameter determination of Chaboche kinematic hardening model using a multi objective Genetic Algorithm, Computational Materials Science. 50 (2011) 1114-1122.

[51] JA Nelder, R Mead. A simplex method for function minimization, The computer journal. 7 (1965) 308.

[52] L Sun, R Wagoner. Proportional and non-proportional hardening behavior of dual-phase steels, Int.J.Plast. 45 (2013) 174-187.